

Accepted Manuscript

Research papers

Monitoring Induced Denitrification During Managed Aquifer Recharge in an Infiltration Pond

Alba Grau-Martínez, Albert Folch, Clara Torrentó, Cristina Valhondo, Carme Barba, Cristina Domènech, Albert Soler, Neus Otero

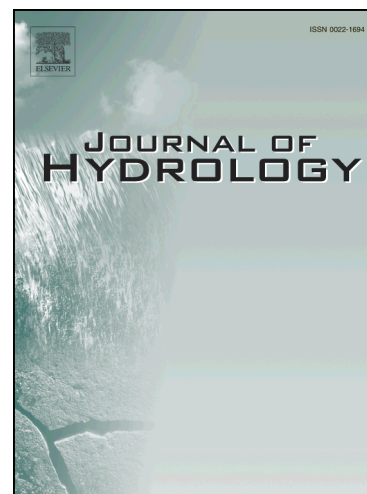
PII: S0022-1694(18)30210-5
DOI: <https://doi.org/10.1016/j.jhydrol.2018.03.044>
Reference: HYDROL 22677

To appear in: *Journal of Hydrology*

Received Date: 27 July 2017
Revised Date: 16 March 2018
Accepted Date: 17 March 2018

Please cite this article as: Grau-Martínez, A., Folch, A., Torrentó, C., Valhondo, C., Barba, C., Domènech, C., Soler, A., Otero, N., Monitoring Induced Denitrification During Managed Aquifer Recharge in an Infiltration Pond, *Journal of Hydrology* (2018), doi: <https://doi.org/10.1016/j.jhydrol.2018.03.044>

This is a PDF file of an unedited manuscript that has been accepted for publication. As a service to our customers we are providing this early version of the manuscript. The manuscript will undergo copyediting, typesetting, and review of the resulting proof before it is published in its final form. Please note that during the production process errors may be discovered which could affect the content, and all legal disclaimers that apply to the journal pertain.



MONITORING INDUCED DENITRIFICATION DURING MANAGED AQUIFER RECHARGE IN AN INFILTRATION POND

Alba Grau-Martínez^a, Albert Folch^{b,c}, Clara Torrentó^{a,d}, Cristina Valhondo^{c,e}, Carme Barba^{b,c},
Cristina Domènech^a, Albert Soler^a, Neus Otero^{a,f}

Monitoring induced denitrification during managed aquifer recharge in an infiltration pond.

A. Grau-Martínez^{1}, A. Folch^{2,3}, C. Torrentó^{1,4}, C. Valhondo^{3,5}, C. Barba^{2,3}, C. Domènech¹,
A. Soler¹, N. Otero^{1,6}*

¹Grup de Mineralogia Aplicada i Geoquímica de Fluids, Departament de Mineralogia, Petrologia i Geologia Aplicada, SIMGEO UB-CSIC, Facultat de Ciències de la Terra, Universitat de Barcelona (UB), C/ Martí i Franquès, s/n - 08028 Barcelona, Spain. albagrau@ub.edu, clara.torrento@ub.edu, cristina.domenech@ub.edu, albertsoler@ub.edu, notero@ub.edu

²Department of Civil and Environmental Engineering (DECA), Universitat Politècnica de Catalunya (UPC), c/Jordi Girona 1-3, 08034 Barcelona, Spain.

³Associated Unit: Hydrogeology Group (UPC-CSIC). carme.barba@upc.edu, cristina.valhondo@upc.edu, folch.hydro@gmail.com

⁴Centre for Hydrogeology and Geothermics, University of Neuchâtel, Rue Emile-Argand 11, 2000 Neuchâtel, Switzerland. clara.torrento@unine.ch

⁵Institute of Environmental Assessment and Water Research (IDAEA), CSIC, c/ Jordi Girona 18, 08034 Barcelona, Spain.

⁶Serra Hunter Fellow, Generalitat de Catalunya, Spain.

(*) Corresponding author: Alba Grau-Martínez

e-mail: albagrau@ub.edu, notero@ub.edu

Fax: +34 93 402 13 40.

Phone: +34 93 403 37 73

Abstract

Managed aquifer recharge (MAR) is a well-known technique for improving water quality and increasing groundwater resources. Denitrification (i.e. removal of nitrate) can be enhanced during MAR by coupling an artificial recharge pond with a permeable reactive layer (PRL). In this study, we examined the suitability of a multi-isotope approach for assessing the long-term effectiveness of enhancing denitrification in a PRL containing vegetal compost. Batch laboratory experiments confirmed that the PRL was still able to enhance denitrification two years after its installation in the infiltration pond. At the field scale, changes in redox indicators along a flow path and below the MAR-PRL system were monitored over 21 months during recharge and non-recharge periods. Results showed that the PRL was still releasing non-purgeable dissolved organic carbon five years after its installation. Nitrate concentration coupled with isotopic data collected from the piezometer network at the MAR system indicated that denitrification was occurring in the saturated zone immediately beneath the infiltration pond, where recharged water and native groundwater mix. Furthermore, longer operational periods of the MAR-PRL system increased denitrification extent. Multi-isotope analyses are therefore proved to be useful tools in identifying and quantifying denitrification in MAR-PRL systems.

Keywords: nitrate reduction, multi-isotope analysis, reactive layer, mixing zone, artificial recharge, field and laboratory experiments.

1. Introduction

Increasing water demands with growing world population and potential water shortages require flexible management strategies to replenish aquifers. The artificial recharge of

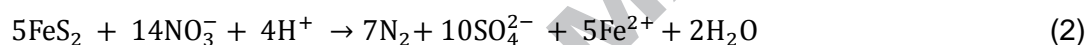
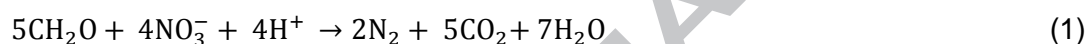
groundwater, commonly known as managed aquifer recharge (MAR), is becoming increasingly important all over the world as a sustainable way of protecting the quality and quantity of groundwater supplies [Bouwer, 2002; Dillon, 2004; Sprenger et al., 2017]. Recharge ponds are one of the most commonly used approaches for MAR. This approach involves surface infiltration through spreading basins or ponds to introduce surface water into the subsurface environment [Bouwer, 2002; Miller et al., 2006].

Common sources of water for MAR in recharge ponds include wastewater effluents (after different stages of treatment) and effluent-receiving rivers [Díaz-Cruz and Barceló, 2008; Maeng et al., 2011], as well as river water and storm water runoff. These sources of water, mainly those from wastewater treatment plants (WWTPs), might contain high levels of ammonium (NH_4^+), whereas those resulting from agricultural activity might have high concentrations of nitrate (NO_3^-) [Schmidt et al., 2011]. Furthermore, oxic conditions promote ammonium nitrification, transforming it to nitrate.

The chemical composition of the infiltrating water in MAR changes due to a combination of physical and biogeochemical processes as the water passes from unsaturated to saturated zones, where it mixes with native groundwater. In some circumstances, these changes can lead to an overall improvement in groundwater quality [Bouwer, 2002; Fox et al., 2006]. Several studies have demonstrated that artificial recharge reduces the concentration of nutrients [Bekele et al., 2011], organic matter [Bekele et al., 2011; Vanderzalm et al., 2006], metals [Dillon et al., 2006; Bekele et al., 2011], pathogens [Dillon et al., 2006], organic contaminants [Dillon et al., 2006; Patterson et al., 2011] and pharmaceutically active compounds (PhACs) [Herber et al., 2004; Valhondo et al., 2014, 2015]. Massmann et al. [2006], investigated changes in redox conditions below an artificial recharge pond in Berlin, and found that the level of PhACs in groundwater was controlled by the transient hydraulic and hydrochemical conditions during artificial recharge. Thus, to increase the quality of recharge water and groundwater, the infiltration pond can be coupled to a permeable reactive layer (PRL), an organic reactive layer at the bottom of the pond [Valhondo et al.,

2014, 2015, 2016] that promotes diverse redox conditions along the recharge path to enhance the degradation of pollutants.

NO_3^- is one of the most abundant pollutants in groundwater [Li et al., 2010; Menció et al., 2016]. Denitrification, a microbe-mediated process in which NO_3^- is converted into dinitrogen gas (N_2), is the main naturally occurring process that decreases NO_3^- concentration in groundwater. Dilution and dispersion also decrease groundwater nitrate concentration, but in contrast to denitrification, they do not lead to mass reduction of the contaminant within an aquifer. Denitrification is carried out by bacteria that use NO_3^- as the terminal electron acceptor when dissolved oxygen (DO), which is energetically more favorable, is unavailable [Knowles, 1982]. Denitrification can be heterotrophic or autotrophic, depending on whether the substrate is organic or inorganic, respectively (Eq.1 and 2).



Denitrification can be enhanced in MAR-PRL pond systems, since adequate residence time and the presence of easily degradable organic carbon promote the activity of heterotrophic denitrifying bacteria. Recent laboratory studies [Grau-Martínez et al., 2017; Gibert et al., 2008] have suggested that low-cost carbon-releasing materials like organic compost, palm tree leaves and wood by-products could induce denitrification. Promoting denitrification by using a reactive layer in a recharge pond requires control mechanisms to test the efficacy of the implemented materials at the field scale.

Multi-isotope analysis, coupled with chemical data, is useful for identifying and even quantifying denitrification processes in aquifers [Mariotti et al., 1988; Aravena and Robertson, 1998; Pauwels et al., 2000, among others]. Denitrification affects the isotope composition of the residual nitrate, resulting in increased levels of the heavy isotopes ^{15}N and ^{18}O [Mariotti et al., 1988; Aravena and Robertson, 1998; Fukada et al., 2003; Kendall et al., 2007]. This change in isotope composition, or isotope fractionation (ϵ), distinguishes denitrification at the field scale from other processes such as dilution, which can also

decrease NO_3^- concentration, but without changing its isotopic value [Clark and Fritz, 1997; Kendall et al., 2007].

Isotopic studies coupled with chemical data are an effective tool to identify and describe denitrification [Aravena and Robertson, 1998; Pauwels et al., 1998, 2000, 2010; Kendall et al., 2007; Otero et al., 2009; among others]. Furthermore, multi-isotopic studies of the solutes involved in denitrification reactions, such as $\delta^{34}\text{S}$ and $\delta^{18}\text{O}$ of dissolved sulphate and $\delta^{13}\text{C}$ of dissolved inorganic carbon, can help determining whether denitrification is promoted by heterotrophic or autotrophic bacteria and identifying the occurrence of secondary processes such as SO_4^{2-} reduction [Mariotti et al., 1988]. Schmidt et al. [2011, 2012] used nitrate isotope ratios to demonstrate the occurrence of denitrification in the infiltrating water during its passage through the first meter of the soil beneath the base of a MAR pond in central coastal California.

In the present work, we monitored denitrification processes in a MAR-PRL system located at Sant Vicenç dels Horts, Barcelona, Spain [Valhondo et al., 2014, 2015, 2016, 2018], which has a layer of vegetal compost at the bottom of the infiltration pond. The aim of the present study is to test the usefulness of a combined isotope analysis and depth specific hydrochemical data to: (i) assess the long-term effectiveness of the reactive layer in promoting denitrification 5 years after its installation; (ii) identify the denitrification processes occurring at different aquifer depths and locations along the saturated zone below the infiltration pond (including the mixing zone between recharge and native groundwater). The methods tested here can be applied in other sites to assess the efficacy of MAR ponds coupled to reactive layer PRL in promoting denitrification.

2. Materials and methods

2.1. Study site description

The field site studied is located 15 km inland from the Mediterranean coast, in the lower valley of the Llobregat Delta (Catalonia, NE Spain). This area is characterized by a Mediterranean climate, with average annual precipitation around 590mm. Precipitation is scarce in winter and summer (monthly average of 37mm) and more frequent during spring (monthly average of 41 mm) and especially autumn (monthly average 77mm). The aquifer consists of Quaternary alluvial sediments, mainly coarse gravel and sand with small clay lenses [Iribar et al., 1997]. The minerals present include quartz, calcite and dolomite, and the solid phase fraction of organic carbon is less than 0.002 (g_{OC}/g_{soil}) [Barbieri et al., 2011]. At this location, the aquifer extends to a depth of 23 to 27 m underground [Valhondo et al., 2014] and is located between 5 and 10 m below the Llobregat river bed, the river and aquifer thus being hydraulically disconnected [Vázquez-Suñé et al., 2007]. The regional groundwater flow direction is from NNW to SSE [Quevauviller et al., 2009], with a natural hydraulic gradient of 2.3‰. Previous pumping tests determined the hydraulic parameters to be $1.4 \times 10^4 \text{ m}^2 \text{ day}^{-1}$ for transmissivity and 0.03 for storage coefficient [Barahona-Palomo et al., 2011].

Groundwater is artificially recharged by infiltrating water from the Llobregat River via a system of pipes and ponds. The river water is collected approximately 2 Km upstream of the MAR system (Molins de Rei inlet) and flows by gravity through a concrete pipe to a decantation pond ($\approx 4,000 \text{ m}^2$). By the time the river reaches the capture point, it has received treated water from more than 50 wastewater treatment plants [Köck-Schulmeyer et al., 2011]. In the decantation pond, the sediments are allowed to settle for approximately 2-4 days before the water is transferred by a concrete pipe to an infiltration pond ($\approx 5,000 \text{ m}^2$) (Fig. 1). The infiltration rate in the infiltration pond ranges from 0.5 to 2 m d^{-1} , whereas insignificant water infiltration occurs in the decantation pond [Valhondo et al., 2014].

A reactive layer was installed at the bottom of the infiltration pond in 2011 to create favorable conditions for the biodegradation of the contaminants present in the infiltration water. The reactive layer ($\approx 65 \text{ cm}$ thick) consists of aquifer sand (49.5% in volume), vegetal compost

from gardens and scrap wood (49.5%), clay ($\leq 1\%$) and iron oxide dust ($\leq 0.1\%$). The components were mixed on site with an excavator until homogeneity was visually evident. The layer was covered with approximately 5 cm of sand to prevent the woody material from floating away. The compost in the reactive layer was added to promote microbial growth and redox conditions by providing organic matter to the infiltration water. The sand was added to provide structural integrity to the layer and guarantee high hydraulic conductivity. Finally, iron oxides and clay, consisting mainly of illite (33 wt%), smectite (16 wt%) and chlorite (9 wt%), were present to provide extra sorption capacity for cationic and anionic contaminants [Valhondo et al., 2014].

The MAR pond undergoes two main operational periods: (1) recharge periods (RPs), with continuous flow from the river to the pond (infiltration water is mainly river water with less than 1.5% contribution from precipitation on average) and (2) non-recharge periods (NRPs), when the pond is dried for operational redevelopment and/or when the infiltration is stopped because the quality of the river water is low. During recharge periods, total saturation conditions are not obtained [Valhondo et al., 2015, 2016].

NRPs are implemented when the control parameters of the infiltration water are exceeded, such as when NH_4^+ concentrations are higher than 1.5 mg L^{-1} , electrical conductivity (EC) is higher than $2000 \text{ } \mu\text{S cm}^{-1}$, river turbidity is greater than 100 NTU and input water turbidity exceeds 25 NTU. NRPs are also implemented when the clogged layer needs to be removed or the upper layer of sand has to be cleaned. During NRPs, the groundwater table declines and the bottom of the pond is exposed to the atmosphere.

A piezometric network consisting of seven piezometers was installed around the recharge MAR system (Fig. 1). Piezometer P1 (screened from 6 to 24 m) is located upstream of the infiltration pond and was used to monitor background groundwater. P3 (screened from 5 to 23 m) is located upstream of the infiltration pond, between the decantation and infiltration ponds, while P8 is located in the middle of the infiltration pond and is composed of three

piezometers screened at different depths (P8.1 from 13 to 15 m, P8.2 from 10 to 12 m and P8.3 from 7 to 9 m). P8.3 was used to evaluate the behavior of the infiltration water through the vadose zone, while P8.1 was used to monitor the recharge at the deepest point of the saturated zone. P2 (completely screened from 6 to 24 m) and P5 (screened from 5 to 21 m) are situated downstream, at the edge of the infiltration pond. Additionally, P9 (screened from 9 to 24 m) and P10 (screened from 6 to 20 m) are located 190 m and 200 m downstream of the infiltration pond, respectively. Therefore, all the monitoring points, except P1 (native groundwater) and P8.3 (infiltration water just after crossing the vadose zone), represent different ratios of recharge water to native groundwater in the aquifer at different travel times. Travel time of the infiltration water from the pond to the piezometers is around 18 to 24 hours for P8.3, nearly 2 days for P2 and P5, 10 days for P10 and P8.1, and more than 20 days for P9 [Valhondo et al., 2014; 2016]

2.2. Sampling surveys

To assess the long-term effectiveness of the PRL, four sampling campaigns were performed using the seven piezometers (Fig. 1) to evaluate nitrate removal under different operational conditions in June 2013, September 2013, July 2014 and March 2015. The monitored period started 5 years after the installation of the PRL. The June 2013 and July 2014 campaigns were performed during RPs, and the other two during NRPs. Figure 2 shows the distribution along time of the operational periods and the sampling campaigns. The system was under RPs for a total of 222 days in 2013 and 213 days in 2014. In 2015, before the March 2015 campaign, the system was under NRPs for almost four months, whereas only two months of non-recharge had occurred before the September 2013 campaign.

Sampling was carried out using depth-specific samplers (bailers). Bailers are considered suitable for measuring groundwater nitrate concentration [Lasagna and De Luca, 2016]. Each piezometer was sampled at three different depths (Fig. 1), which were selected according to the stratigraphic profiles. A layer with high transmissivity was identified in the

middle depth of all the piezometers. This layer is composed of polygenic gravel and large-sized gravel with medium fine sandy matrix. Although some sampling protocols [ENSAT, 2012] do not deem it necessary to purge piezometers in aquifers with high transmissivity such as that of Sant Vicenç dels Horts ($1.4 \times 10^4 \text{ m}^2 \text{ day}^{-1}$), we still purged the piezometers prior to sampling by removing well water three times at each specific depth. During the four sampling campaigns, samples from the Llobregat River were also collected, sometimes more than once on the same day.

Physicochemical parameters (pH, temperature (T) and EC) were measured *in situ*, using a Multi 3410 multi-parameter (WTW, Weilheim, Germany). Samples for measuring major cations were filtered through 0.2- μm Millipore® filters, preserved by the addition of 1% HNO_3^- and stored in polyethylene bottles at 4°C until analysis. Samples for the analysis of major anions (Cl^- , NO_3^- , NO_2^- and SO_4^{2-}) and isotope ratios ($\delta^{15}\text{N}_{\text{NO}_3}$, $\delta^{18}\text{O}_{\text{NO}_3}$, $\delta^{34}\text{S}_{\text{SO}_4}$, $\delta^{18}\text{O}_{\text{SO}_4}$ and $\delta^{13}\text{C}_{\text{HCO}_3}$) were filtered through 0.2- μm Millipore® filters and stored in polyethylene bottles. Samples for measuring NO_3^- isotopes were kept frozen until analysis, while those for $\delta^{18}\text{O}_{\text{H}_2\text{O}}$ and $\delta^2\text{H}_{\text{H}_2\text{O}}$ measurements were collected in glass flasks and filtered through 0.45- μm Millipore® filters. For isotope analyses, samples were taken only from the middle depth of each piezometer. Samples for the analysis of non-purgeable dissolved organic carbon (NPDOC) were collected in muffled (450°C , 4.5 hours) glass bottles, filtered through 0.45- μm Millipore® filters, acidified to pH 3 with hydrochloric acid and stored at 4°C until analysis. To measure dissolved inorganic carbon (DIC), samples were collected in glass bottles, filtered through 0.45- μm Millipore® filters and analyzed within a day.

2.3. Laboratory experiments

Batch experiments were performed with material extracted in 2013 from the PRL of the MAR pond system. The substrate was used within a few hours after extraction without any pre-treatment. Experiments were performed in triplicate, using 20 g of the PRL material and 400 mL of groundwater from the Llobregat aquifer (from P2) spiked with 0.80 mM of NO_3^- to

evaluate the denitrification potential of the vegetal compost. The experiments were run in sterilized 500-mL glass bottles previously purged with N₂ for 15 minutes in a glove box in an argon atmosphere to minimize the O₂ level. Experimental oxygen partial pressure in the glove box was maintained between 0.1 and 0.3% O₂ and continuously monitored using an oxygen partial pressure detector (Sensotran, Gasvisor 6) with an accuracy of ± 0.1% O₂. Batch experiments were manually shaken once a day and aqueous samples (5 mL) were collected daily using sterilized syringes. A ratio of solution/solid material at 90% of the initial value was maintained.

The experiments were performed to check the reactivity of the extracted material and also to estimate the isotopic fractionation (ε) of N and O.

The NO₃⁻ pseudo-first order degradation rate constants (k') were calculated using Eq. (3), where C₀ and C_t are the initial NO₃⁻ concentration and the NO₃⁻ concentration at time t, respectively.

$$C_t = C_0 e^{-k't} \quad (3)$$

Isotopic fractionation during denitrification can be expressed as a Rayleigh distillation process Eq. (4), from which the isotopic fractionation factor (α) can be obtained [Mariotti et al., 1988; Aravena and Robertson, 1998].

$$\ln\left(\frac{R_t}{R_0}\right) = (\alpha - 1) \ln\left(\frac{C_t}{C_0}\right) \quad (4)$$

where C₀ and C_t are the initial and residual NO₃⁻ concentration, respectively (mmol L⁻¹), and R₀ and R_t denote the ratios of heavy to light isotopes at the initial time and time t, respectively, which are calculated according to Eq. (5).

$$R = \left[\left(\frac{\delta}{1000}\right) + 1\right] \quad (5)$$

Where δ is the isotopic composition of δ¹⁵N and δ¹⁸O (‰). The term (α - 1) was calculated from the slope of the regression line in the double-logarithmic plots [ln(R_t/R₀)] vs. [ln(C_t/C₀)],

according to Eq. (5), and converted into isotope fractionation (ϵ_N and ϵ_O) following Eq. (6).

$$\epsilon = 1000 \times (\alpha - 1) \quad (6)$$

The Rayleigh equation applies to closed system conditions; therefore, isotopic fractionation is commonly calculated in laboratory experiments where conditions are well constrained, no other sinks affect the NO_3^- pool and the concentration and isotopic composition of NO_3^- can be considered exclusively determined by NO_3^- reduction.

2.4. Analytical methods

Concentrations of major anions (Cl^- , NO_2^- , NO_3^- , and SO_4^{2-}) were determined by high performance liquid chromatography (HPLC) using a WATERS 515 HPLC pump, an IC-PAC anions column and a WATERS 432 detector. Cation concentrations were determined by inductively coupled plasma-optical emission spectrometry (ICP-OES, Perkin-Elmer Optima 3200 RL). NPDOC was measured by organic matter combustion using a MULTI N/C 3100 Analytik Jena carbon analyzer. DIC concentrations were analyzed by titration (METROHM 702 SM Titrino). Chemical analyses were conducted at the "Centres Científics i Tecnològics" of the University of Barcelona (CCiT-UB).

The $\delta^{15}\text{N}$ and $\delta^{18}\text{O}$ of dissolved NO_3^- were measured using a modified cadmium reduction method of Mclvin and Altabet [2005] and Ryabenko et al. [2009]. Briefly, NO_3^- was converted into nitrite through a spongy cadmium reduction and then to nitrous oxide using sodium azide in an acetic acid buffer. Simultaneous $\delta^{15}\text{N}$ and $\delta^{18}\text{O}$ analysis of the N_2O produced was carried out with a PreCon system (Thermo Scientific) coupled to a Finnigan MAT-253 Isotope Ratio Mass Spectrometer (IRMS, Thermo Scientific). For $\delta^{34}\text{S}$ and $\delta^{18}\text{O}$ analyses, dissolved SO_4^{2-} was precipitated as BaSO_4 by adding BaCl_2 after acidifying the sample with HCl and boiling it to prevent BaCO_3 precipitation, following standard methods [Dogramaci et al., 2001]. $\delta^{34}\text{S}$ was analyzed with a Carlo Erba elemental analyzer (EA)-Finnigan Delta C

IRMS, while $\delta^{18}\text{O}$ was analyzed in duplicate with a ThermoQuest high temperature conversion EA (TC/EA) coupled in continuous flow with a Finnigan MAT Delta C IRMS. For $\delta^{13}\text{C}_{\text{DIC}}$ analysis, carbonates were precipitated by adding a NaOH-BaCl₂ solution and isotope ratio was measured on a Gas-Bench II-MAT-253 IRMS (Thermo Scientific). $\delta^2\text{H}_{\text{H}_2\text{O}}$ and $\delta^{18}\text{O}_{\text{H}_2\text{O}}$ were analyzed by Wavelength-Scanned Cavity Ringdown Spectroscopy (WS-CRDS) using L2120-i Picarro®. Total C, total N, $\delta^{15}\text{N}$ and $\delta^{13}\text{C}$ from the PRL material were measured using Carbo Erba EA-Finnigan Delta C IRMS. Isotope ratios were calculated using both international and internal laboratory standards. Notation was expressed in terms of δ relative to the international standards (V-SMOW for $\delta^{18}\text{O}$ and $\delta^2\text{H}$, atmospheric N₂ for $\delta^{15}\text{N}$, V-CDT for $\delta^{34}\text{S}$ and V-PDB for $\delta^{13}\text{C}$). The reproducibility of the samples was $\pm 1\text{‰}$ for the $\delta^{15}\text{N}$ of NO₃⁻, $\pm 1.5\text{‰}$ for the $\delta^{18}\text{O}$ of NO₃⁻, $\pm 0.2\text{‰}$ for the $\delta^{34}\text{S}$ of SO₄²⁻, $\pm 0.5\text{‰}$ for the $\delta^{18}\text{O}$ of SO₄²⁻, $\pm 0.2\text{‰}$ for the $\delta^{13}\text{C}$ of DIC, $\pm 0.2\text{‰}$ for the $\delta^{18}\text{O}$ of H₂O and $\pm 1\text{‰}$ for the $\delta^2\text{H}$ of H₂O. Samples for isotopic analyses were prepared at the “Mineralogia Aplicada i Geoquímica de Fluids” laboratory and analyzed at CCiT-UB, except water isotopes, which were analyzed at the University of Málaga.

3. Results and discussion

3.1. Laboratory experiments

Total N and C content as well as the $\delta^{15}\text{N}$ and $\delta^{13}\text{C}$ of the reactive layer material are shown in the Supplementary Material (Table S1). Results of the chemical and isotopic characterization of the batch experiments are detailed in the Supplementary Material (Table S2).

Complete NO₃⁻ reduction was achieved within eleven days in the batch experiments (Fig. 3), with a slight transient increase in NO₂⁻ concentration (up to 0.07 mM). Nitrate reduction in previous batch experiments performed with fresh commercial compost was accompanied by a significant initial release of NO₃⁻ (up to 2.5 mM) and transient NO₂⁻ production (up to 0.12

mM) [Grau-Martínez et al., 2017]. By comparison, the compost used in the present batch experiments, extracted from the PRL two years after its installation, did not release NO_3^- and produced a lower increase in NO_2^- concentration.

Denitrification in both sets of batch experiments followed pseudo-first-order kinetics and an initial lag phase of 6-7 days with a lower degradation rate was observed. The observed k' values were 0.21 ± 0.01 and $0.83 \pm 0.06 \text{ d}^{-1}$ with the PRL material and 0.17 ± 0.02 and $0.67 \pm 0.01 \text{ d}^{-1}$ with the fresh compost for the lag and main phases, respectively. Although highly similar, degradation rates were slightly higher for the PRL material than for the fresh compost. These results demonstrated that the compost from the PRL still had denitrification potential two years after its installation.

The isotopic fractionations obtained were -10.4‰ for ϵN and -13.8‰ for ϵO , with a $\epsilon\text{N}/\epsilon\text{O}$ ratio of 0.75 (Fig. 4a and 4b). The ϵN and ϵO values obtained in this study were similar to those from previous laboratory experiments using fresh commercial compost ($\epsilon\text{N} = -10.8\text{‰}$ and $\epsilon\text{O} = -9.0\text{‰}$ [Grau-Martínez et al., 2017]), also falling within the range of laboratory values for heterotrophic denitrification reported in the literature (from -8.6‰ to -16.2‰ for ϵN and from -4‰ to -13.8‰ for ϵO [Knöller et al., 2011; Carrey et al., 2013]).

The obtained C and N isotope fractionations associated with denitrification induced by the two-year-old PRL material enables a more accurate quantification of the enhanced reduction in NO_3^- levels in the aquifer.

3.2. Field study

3.2.1. Hydrochemical characterisation

Results of the chemical characterization of the field samples are detailed in the Supplementary Material (Table S3). For all the analyzed samples, pH values ranged between 6.98 and 7.60, HCO_3^- concentrations between 223 and 408 mg L^{-1} and EC from 991 to 1653 $\mu\text{S cm}^{-1}$. There were no significant differences in the concentrations of major cations between the piezometers among the four sampling campaigns.

Groundwater underneath the infiltration pond can be considered a mixture of recharge water and native groundwater. Samples clustered in the $\text{HCO}_3\text{-Cl-Ca-Na}$ hydrochemical facies, with negligible differences among the sampling campaigns (Fig. S1).

3.2.2. Sources of groundwater recharge

Results of the isotopic characterization of the field samples are detailed in the Supplementary Material (Table S4). $\delta^2\text{H}$ and $\delta^{18}\text{O}$ values of the infiltration water (river water) and groundwater sampled during RPs (June 2013 and July 2014) mostly plotted along the Local Meteoric Water Line (LMWL) (Fig. 5). The LMWL was calculated with data from the Global Network of Isotopes in Precipitation (GNIP) obtained from stations 0818001 and 0818002 in Barcelona (IAEA/WMO, 2017). Isotope ratios are lower than the weighted mean long-term isotopic composition of precipitation in Barcelona ($\delta^2\text{H} = -31.16\text{‰}$, $\delta^{18}\text{O} = -5.3\text{‰}$), but in agreement with the values obtained with the surface water of the Lower end of the Llobregat River [Otero et al., 2008] and samples from the Llobregat aquifer [Solà, 2009]. The results confirmed that river water is the main source of recharge in the aquifer and indicate that evaporation is not an important process in the pond and/or the unsaturated zone. Lastly, the range of $\delta^2\text{H}$ and $\delta^{18}\text{O}$ values showed that only one recharge flow system is involved in the aquifer recharge. Accordingly, Valhondo et al. [2015], using electrical conductivity and 1,1,2-trichloroethane content as tracers, estimated the contribution of the infiltration water on the monitoring points and showed that samples collected in P2, P5, P8.3 and P10 comprised primarily infiltrated water, whereas wells P8.2, P8.1 and P9 displayed a mixture of infiltration water and local groundwater (P1), although the concentrations were closer to the infiltration water composition.

3.3. Changes in redox sensitive indicators

The evolution of the concentration of NO_3^- and NPDOC in the saturated zone along the flow path, during both RPs and NRPs, is shown in Figure 6. The results of major anions (Cl^- , SO_4^{2-} , HCO_3^-) are shown in the Supplementary Material (Fig. S2).

For assessing the effect of MAR, the chemical composition of groundwater collected upstream of the infiltration pond (P1, which represents native groundwater not affected by the recharge) was compared to that of the piezometers affected by recharge water. The concentrations of major anions in P1 samples remained almost constant with depth and time (Fig. S2). The influence of river water is clearly observed in the piezometers located closer to the infiltration pond (P8, P2 and P5) during RP and to a lesser extent during NRPs. Piezometers located furthest from the infiltration pond (P9 and P10) are less influenced by river water chemistry. Overall, no significant changes with depth were observed during both RP and NRPs.

NPDOC concentrations at the piezometers downstream of the infiltration pond generally ranged between those for native groundwater and those for river water (Fig. 6) during both RP and NRP, being generally lower during NRPs. Higher NPDOC concentrations were detected in some samples (e.g. P2 in July 2014, P3 and P8 in September 2013, P8 in March 2015). These results suggest that the reactive layer was still releasing NPDOC five years after installation. Average higher NPDOC concentration was detected in September 2013 (two months of non-recharge before sampling) than in March 2015 (four months of non-recharge before sampling), indicating that the duration of recharge conditions had a significant effect.

NO_3^- concentration (measured as mg of $\text{NO}_3^- \text{L}^{-1}$) in native groundwater (P1) ranged from 4.2 to 9.8 mg L^{-1} with a median value of 5.6 (Table S3). Additional river water data show NO_3^- contents between 4.5 and 17.4 mg L^{-1} (Table S5). It should be noted that NO_3^- and NH_4^+ concentrations vary considerably in rivers with effluents from WWTPs, even among samples collected on the same day. During the RPs a significant decrease in NO_3^- concentration was

observed in the piezometers located close to the infiltration pond (P2 and P5), especially in the June 2013 sampling, which showed complete NO_3^- reduction at some depths highlighting the ability of the MAR-PRL system to enhance nitrate reduction (Fig. 6). During the July 2014 RP, a decrease in NO_3^- concentration was also observed downstream of the pond but to a lesser extent. During NRPs, NO_3^- concentrations at the downstream piezometers were generally within native groundwater and river water samples, although slightly lower NO_3^- concentrations were seldom detected suggesting that NO_3^- reduction was maintained to some extent.

Fe concentrations in samples downstream of the infiltration pond were generally lower than that in the native groundwater (P1) (Table S3). No significant variations between the sampling campaigns were observed (values ranged from 0.2 to 1.0 μM), except for an important increase at P5 during the June 2013 RP (up to 3.7 μM) probably arising from more reducing conditions occurring. The solubility of Fe(III)-oxyhydroxides, which usually affects Fe concentration in groundwater, increases under more reducing conditions, thereby increasing aqueous Fe concentration.

Overall, the observed changes in redox indicators suggested that the PRL installed in 2011 was still releasing organic matter and promoting reducing conditions to varying extents below the infiltration pond.

3.4. Denitrification during artificial recharge

Nitrate isotope composition was measured in a subset of these samples based on NO_3^- concentrations (Table S4). Figure 7 shows the $\delta^{15}\text{N}_{\text{NO}_3}$ and $\delta^{18}\text{O}_{\text{NO}_3}$ values of dissolved nitrate at the piezometers, as well as the isotope composition of the main potential sources of nitrate: nitrate fertilizers, ammonium fertilizers, soil nitrate and animal manure or sewage [Vitòria et al., 2004; Kendall et al., 2007; Xue et al., 2009]. The range of $\delta^{18}\text{O}$ of NO_3^- for ammonium fertilizers, soil nitrogen and manure/sewage plotted in Figure 7 (+1.93‰ to +3.13‰) was estimated according to Eq.7 [Anderson and Hooper, 1983; Kendall et al.,

2007], where $\delta^{18}\text{O}_{\text{H}_2\text{O}}$ corresponds to the range measured in Sant Vicenç dels Horts groundwater samples and $\delta^{18}\text{O}_{\text{O}_2}$ to atmospheric O_2 (+23.5‰ [Horibe et al., 1973]).

$$\delta^{18}\text{O}_{\text{NO}_3} = \frac{2}{3}(\delta^{18}\text{O}_{\text{H}_2\text{O}}) + \frac{1}{3}(\delta^{18}\text{O}_{\text{O}_2}) \quad (7)$$

Native groundwater (P1) showed $\delta^{15}\text{N}$ and $\delta^{18}\text{O}$ values ranging from +13.0 to +17.5‰ and from +2.8 to +9.7‰, respectively. The nitrate isotope ratios of the samples from the piezometers located downstream of the pond ranged from +9.5 to +26.7‰ (averaging +18.4‰) for $\delta^{15}\text{N}$ and from +3.5 to +16.6‰ (averaging +9.5‰) for $\delta^{18}\text{O}$ (Table S4). All samples presented isotope ratios compatible with those for soil organic nitrogen and sewage/manure. The mixed groundwater samples showed a positive correlation ($r^2=0.55$) between $\delta^{15}\text{N}_{\text{NO}_3}$ and $\delta^{18}\text{O}_{\text{NO}_3}$ and were aligned following a $\epsilon\text{N}/\epsilon\text{O}$ ratio of 1.5 (Fig. 7), which is consistent with denitrification [Kendall et al., 2007]. The $\epsilon\text{N}/\epsilon\text{O}$ ratio reported in the literature for denitrification in groundwater ranges from 1.3 to 2.1 [Böttcher et al., 1990; Cey et al., 1999; Mengis et al., 1999; DeVito et al., 2000; Lehmann et al., 2003; Fukada et al., 2003].

Most samples collected during the RPs followed the denitrification trend, with higher $\delta^{15}\text{N}_{\text{NO}_3}$ and $\delta^{18}\text{O}_{\text{NO}_3}$ during the July 2014 sampling. During NRPs also a different behavior was observed in the two surveys, with lower isotopic values in March 2015 and high values in the September 2013 sampling. However, it should be noted that in both September 2013 and July 2014 samplings, high $\delta^{15}\text{N}$ and $\delta^{18}\text{O}$ values were also measured in river water. The high variability of NO_3^- contents in river water samples even on the same day (Table S5) could explain the particularly high isotope ratios measured in September 2013 and July 2014. Accordingly, Sine [2017] reported that NO_3^- isotopes values in a highly impacted river are not conservative, even when NO_3^- contents do not change. These authors studied the Grand River (south western Ontario, Canada), which receives high NO_3^- loading from point (urban WWTPs) and non-point sources (agricultural manure and fertilizer) and suggested that river metabolism influences rapid isotopic changes.

ϵN and ϵO values allow quantifying at field scale NO_3^- losses due to denitrification independently of dilution effects on NO_3^- concentrations [Mariotti et al., 1981; Böttcher et al., 1990; Fukada et al., 2003; Otero et al., 2009; Torrentó et al., 2011]. With the ϵ values obtained in laboratory experiments, the percentage of denitrification at the field scale can be calculated according to Eq. (8) using either ϵN or ϵO , or both.

$$\text{DEN (\%)} = \left[1 - \frac{[\text{NO}_3^-]_{\text{residual}}}{[\text{NO}_3^-]_{\text{initial}}} \right] \times 100 = \left[1 - e^{\left(\frac{\delta_{(\text{residual})} - \delta_{(\text{initial})}}{\epsilon} \right)} \right] \times 100 \quad (8)$$

The extent of denitrification enhanced by the MAR-PRL system was estimated for each sampling campaign. The isotope composition of the native groundwater (P1) for each campaign was used as the initial value, and the ϵ values were obtained from the batch experiments with the two-year-old PRL material (-10.4‰ for ϵN and -13.8‰ for ϵO , with an $\epsilon\text{N}/\epsilon\text{O}$ ratio of 0.75) (Fig. 8).

This approximation shows that during both RPs, the NO_3^- reduction percentage was similar with a maximum value around 30% - 40%. Complete denitrification at some depths of P2 and P5 was observed in samples collected in June 2013 (Fig. 6), but isotopic values were not determined due to the low NO_3^- concentration. Denitrification was enhanced in the piezometers located closer to the infiltration pond (P2). In all campaigns, the isotope composition of P8.2 was very similar to that of P1, indicating that denitrification was not occurring. Since isotopes in samples at different depths were not determined, the cause of variations in NO_3^- concentration along depth at P8 could be either due to denitrification or other process (e.g., mixing). Comparing the two RP sampling campaigns, the June 2013 samples presented a slightly higher level of denitrification, most probably because the system was under almost continuous operation since January 2012 (except for 30 days in August 2012, 24 days in February-March 2013 and 5 days in April 2013). The MAR system was stopped from 22nd June to 1st July, 10 days before the July 2014 sampling campaign. The longer operational period before the June 2013 campaign could have induced a well-

developed denitrifying microbial community, with the bacteria being more concentrated in the areas receiving more recharge water, such as P2 and P5. Li et al. [2013], simulating the infiltration zone of a MAR system, showed that microbial communities reached stability after 3-4 months of operation.

During NRPs, the percentage of denitrification was very low (<20%) in all the samples, except those from P2 (30-60%), which was one of the piezometers most affected by recharge water [Valhondo et al., 2014] (Fig. 8). All the samples collected in March 2015, including P2, showed the lowest percentage of denitrification among all the sampling campaigns. The September 2013 campaign was performed after a year of almost continuous recharge (Fig. 2) followed by less than two months of non-recharge, whereas the March 2015 campaign was undertaken after almost four months of non-recharge. Differences in the percentage of denitrification among the P2 samples collected from both NRPs indicate that the bacteria grow during RPs were still denitrifying even when the MAR pond was under non-recharge, but became less active with time in the absence of a carbon source [Rodríguez-Escales et al., 2016a; 2016b].

Results indicate that time of operation is a key issue to enhance denitrification in the MAR-PRL system. However, in practical terms it is difficult to accomplish due to day by day management issues (low quality river water, maintenance, etc.). In this regard, chaotic advection could be a good technology to keep high denitrification rates as well as other pollutant degradation in both RPs and NRPs as stated in Rodríguez-Escales et al. [2017].

3.5. Additional isotope data

On the one hand, the redox conditions induced in a MAR-PRL system determine the degradation of different contaminants. In the case of mixtures of emerging organic contaminants, for example, increasing the variability of redox conditions is crucial since the individual degradation of these compounds depends on specific redox conditions [e.g.

Barbieri et al., 2011; Liu et al., 2013]. Characterizing the redox conditions achieved in the studied MAR-PRL system is thus critical.

Monitoring the redox sensitive indicators and the nitrate isotope data suggested that the organic matter released by the PRL was promoting reducing conditions to varying extents, at least to nitrate reduction conditions, and probably iron reductions conditions occasionally in P5. The isotope composition of SO_4^{2-} ($\delta^{34}\text{S}_{\text{SO}_4}$ and $\delta^{18}\text{O}_{\text{SO}_4}$) was analyzed to assess the occurrence of sulfate-reducing conditions. Sulfate reduction should produce a decrease in the SO_4^{2-} concentration and an increase in the $\delta^{34}\text{S}_{\text{SO}_4}$ values of the dissolved SO_4^{2-} . The isotope composition of the dissolved SO_4^{2-} in mixed groundwater samples was only analyzed for the June 2013 and September 2013 campaigns. Values ranged from +6.7 to +10.6‰ for $\delta^{34}\text{S}$ and from +9.0 to +11.1‰ for $\delta^{18}\text{O}$ (Fig. 9). Similar values were obtained for the river water and native groundwater samples. Most of the mixed groundwater samples gave values within the range obtained for sewage [Otero et al., 2008] (Fig. 9), indicating that the vast majority of SO_4^{2-} came from sewage, which is consistent with the conclusions drawn from the NO_3^- isotope results regarding potential NO_3^- sources.

The narrow range of the $\delta^{34}\text{S}_{\text{SO}_4}$ and $\delta^{18}\text{O}_{\text{SO}_4}$ values obtained suggests a lack of SO_4^{2-} reduction. It can thus be concluded that the NPDOC released by the reactive layer produces variable redox conditions in the saturated zone along the flow path, leading mainly to the reduction of NO_3^- , as well as iron under certain conditions, but not of SO_4^{2-} . Results indicate that time of operation is a key issue to modify redox conditions as well as pollutant degradation in the MAR-PRL system.

On the other hand, the isotopic composition of dissolved inorganic carbon $\delta^{13}\text{C}_{\text{HCO}_3}$ can provide information about the denitrification reaction [Aravena and Robertson, 1998]. However, in the studied site, due to the aquifer lithology, groundwater contained high concentrations of bicarbonate (median value of $325 \pm 25 \text{ mg L}^{-1}$ in P1 for the four sampling campaigns) that could buffer any change in the $\delta^{13}\text{C}_{\text{HCO}_3}$ isotope ratio linked to denitrification.

The $\delta^{13}\text{C}_{\text{HCO}_3}$ values in P1 samples (native groundwater) averaged $-13.2\pm 1\%$, which is in agreement with the known range of $\delta^{13}\text{C}_{\text{HCO}_3}$ for groundwater (-16% to -11% [Vogel and Ehhalt, 1963]). Mixed groundwater samples displayed $\delta^{13}\text{C}_{\text{HCO}_3}$ values close to that of P1 samples (between -13.8 and -12.0% , with a median value of -12.7%), except three samples collected in the June 2013 campaign (RP) (that had values ranging from -11.1 to -9.9%) (Fig. 10). As expected, the role of organic matter oxidation in the observed denitrification processes was not evident from the $\delta^{13}\text{C}_{\text{HCO}_3}$ data due to the buffering effect of the bicarbonate.

4. Conclusions

We evaluated the feasibility of a multi-isotope approach for assessing the efficacy of the MAR-PRL system of Sant Vicenç dels Horts in promoting denitrification in the groundwater below the infiltration pond. Similarities in the hydrochemical data (except for NO_3^- contents, which decreased during recharge periods in mixed groundwater) of river water, native groundwater and mixed groundwater demonstrated a unique recharge flow system. Changes in the redox indicators with depth and along the flow path during recharge and non-recharge periods confirmed that the reactive layer was still releasing NPDOC five years after installation. NO_3^- concentrations decreased during recharge periods especially in the piezometers closest to the infiltration pond, while aqueous Fe concentrations increased in the piezometers with lower NO_3^- concentrations, however, SO_4^{2-} reduction was not observed. Isotope data revealed that denitrification mainly occurred in the area under the infiltration pond. The piezometers closest to the MAR-PRL, P2 and P5, showed higher levels of denitrification than the other piezometers. Importantly, denitrification was enhanced by a more continuous recharge of the MAR-PRL system, probably because microbial communities become stable after 3-4 months of continuous operation. Although a more detailed field sampling survey is needed to determine the real extent of denitrification at the

field scale, the results of this study show the usefulness of a multi-isotope approach in identifying denitrification in MAR-PRL systems.

Acknowledgements

This study was funded by the projects REMEDIATION [ref. CGL2014-57215-C4-1-R] and ISOTEC [CGL2017-87216-C4-1-R], financed by the Spanish Ministry of Economy AEI/FEDER, EU, the project MAG [Catalan Government, ref. 2014SGR-1456] and the European Union projects WADIS-MAR [European Commission, ref. ENPI/2011/280-008] and MARSOL [European Commission, FP7-ENV-2013-WATER-INNO-DEMO]. We thank the editor and three anonymous reviewers for comments that improved the quality of the manuscript.

References

Anderson, K.K., Hooper, A.B., (1983). O₂ and H₂O are each the source of O in NO₂ produced from NH₃ by Nitrosomas ¹⁵N-NMR evidence. FEBS Lett. 64, 236-240.

Aravena, R., Robertson, W.D., (1998). Use of multiple isotope tracers to evaluate denitrification in ground water: Study of nitrate from a large-flux septic system plume. Ground Water 36, 975-982.

Barahona-Palomo, M., Barbieri, M., Fernàndez-Garcia, D., Pedretti, D., Sanchez-Vila, X., Valhondo, C., Queralt, E., Massana, J., Hernández, M., Tobella, J., (2011). Caracterització del Sistema de Recàrrega de Sant Vicenç dels Horts: Projecte RASA, Informe Fase 2, Barcelona: CUADLL.

Barbieri, M., Carrera, J., Sanchez-Vila, X., Ayora, C., Cama, J., Köck-Schulmeyer, M., López de Alda, M., Barceló, D., Tobella Brunet, J., Hernández García, M., (2011). Microcosm experiments to control anaerobic redox conditions when studying the fate of organic micropollutants in aquifer material. J. Contam. Hydrol. 126 (3-4): 330-345.

Bekele, E., Toze, S., Patterson, B., Higginson, S., (2011). Managed aquifer recharge of treated wastewater: water quality changes resulting from infiltration through the vadose zone. Water Res. 45 (17), 5764-5772.

Böttcher, J., Strelbel, O., Voerkelius, S., Schmidt, H.L., (1990). Using isotope fractionation of nitrate-nitrogen and nitrate-oxygen for evaluation of microbial denitrification in sandy aquifer. *J. Hydrol.* 114, 413-424.

Bouwer, H., 2002. Artificial recharge of groundwater: hydrogeology and engineering. *Hydrogeol. J.* 10, 121-142.

Carrey, R., Otero, N., Soler, A., Gomez-Alday, J.J., Ayora, C., (2013). The role of Lower Cretaceous sediments in groundwater nitrate attenuation in central Spain: Column experiments. *Appl. Geochem.* 32, 142-152.

Cey, E.E., Rudolph, D.L., Aravena, R., Parkin, G., (1999). Role of the riparian zone in controlling the distribution and fate of agricultural nitrogen near a small stream in southern Ontario. *J. Contam. Hydrol.* 37, 45-67.

Clark, I.D., Fritz, P., (1997). *Environmental Isotopes in Hydrogeology*. Lewis Publishers, New York (352 pp.).

Cravotta, C.A., (1997). Use of stable isotopes of carbon, nitrogen and Sulphur to identify sources of nitrogen in surface waters in the lower Susquehanna River Basin, Pennsylvania. U.S. Geological Survey Water-Supply Paper. 2497.

Devito, K.J., Fitzgerald, D., Hill, A.R., Aravena, R., (2000). Nitrate dynamics in relation to lithology and hydrologic flow path in a river riparian zone. *J. Environ. Qual.* 29, 1075-1084.

Díaz-Cruz, M.S., Barceló, D., (2008). Trace organic chemicals contamination in ground water recharge. *Chemosphere* 72 (3): 333-342.

Dillon, P.J., (2004). Future management of aquifer recharge. *Hydro. Geol. J.* 13 (1), 313-316.

Dillon, P., Pavelic, P., Toze, S., Rinck-Pfeiffer, S., Martin, R., Knapton, A., Pidsley, D., (2006). Role of aquifer storage in water reuse. *Desalination* 188 (1-3), 123-134.

Dogramaci, S.S., Herczeg, A.L., Schi, S.L., Bone, Y., (2001). Controls on $\delta^{34}\text{S}$ and $\delta^{18}\text{O}$ of dissolved sulfate in aquifers of the Murray Basin, Australia and their use as indicators of flow processes. *Appl. Geochem.* 16, 475-488

ENSAT (Enhancement of Soil Aquifer Treatment), (2012). Modelo hidrogeológico: Modelo conceptual de flujo en el sistema de recarga de Sant Vicenç dels Horts, Barcelona: ENSAT.

Fox, P., et al. 2006. *Advances in Soil Aquifer Treatment Research for Sustainable Water Reuse*. Awwa Research Foundation: Denver, 200.

Fukada, T., Hiscock, K., Dennis, P.F., Grischek, T., (2003). A dual isotope approach to identify denitrification in groundwater at river-bank infiltration site. *Water Res.* 37, 3070-3078.

Gibert, O., Pomierny, S., Rowe, I., Kalin, R.M., (2008). Selection of organic substrates as potential reactive materials for use in a denitrification permeable reactive barrier (PRB). *Bioresources Technol.* 99, 7587-7596.

Grau-Martínez, A., Torrentó, C., Carrey, R., Rodríguez-Escales, P., Domènech, C., Ghiglieri, G., Soler, A., Otero, N., (2017). Feasibility of two low-cost organic substrates for inducing denitrification in artificial recharge ponds: Batch and flow-through experiments. *J. Contam. Hydrol.* 198, 48-58

Heberer, T., Mechlinski, A., Franck, B., Knappe, A., Massmann, G., Pekdeger, A., Fritz, B., (2004). Field studies on the fate and transport of pharmaceutical residues in bank filtration. *Ground Water Monit. Remediat.* 24 (2), 70-77.

Horibe, Y., Shigehara, K., Takakuwa, Y., (1973). Isotope separation factors of carbon dioxide water system and isotopic composition of atmospheric oxygen. *J. Geophys. Res.* 78, 2625-2629.

IAEA/WMO (2017). *Global Network of Isotopes in Precipitation. The GNIP Database*. Accessible at: <http://www.iaea.org/water>

Iribar, V., Carrera, J., Custodio, E., Medina, A., (1997). Inverse modelling of seawater intrusion in the Llobregat delta deep aquifer. *J. Hydrol* 198 (1-4): 226-244.

Kendall, C., Elliott, E.M., Wankel, S.D., (2007). Tracing anthropogenic inputs of nitrogen to ecosystems. (Chapter 12). In: Michener, R.H., Lajtha, K., (Eds), *Stable isotopes in Ecology and Environmental Science*, second ed. Blackwell Publishing, pp. 375-449.

Knöller, K., Vogt, C., Haupt, M., Feisthauer, S., Richnow, H.H., (2011). Experimental investigation of nitrogen and oxygen isotope fractionation in nitrate and nitrite during denitrification. *Biogeochemistry* 103, 371-384.

Knowles, R., (1982). Denitrification. *Microbiol. Rev.* 46, 43-70.

Köck-Schulmeyer, M., Ginebreda, A., Postigo, C., López-Serna, R., Pérez, S., Brix, R., Llorca, M., MLd Alda, Petrovic, M., Munné, A., Tirapu, L., Barceló, D., (2011). Wastewater reuse in Mediterranean semi-arid areas: the impact of discharges of tertiary treated sewage on the load of polar micro pollutants in the Llobregat River (NE Spain). *Chemosphere* 82(5): 670-678.

Krouse, H.R., Mayer, B., (2000). Sulphur and oxygen isotopes in sulphate. In: Cook, P.G., Herczeg, A.L. (Eds.), *Environmental Tracers in Subsurface Hydrology*. Kluwer Academic Press, Boston, pp.195-231.

Lasagna, M., De Luca, D.A., (2016). The use of multilevel sampling techniques for determining shallow aquifer nitrate profiles. *Environ. Sci. Pollut. Res.* 23 (20) 20431-20448.

Lehmann, M.F., Reichert, P., Bernasconi, S.M., Barbieri, A., McKenzie, J.A., (2003). Modelling nitrogen and oxygen isotope fractionation during denitrification in a lacustrine redox-transition zone. *Geochim. Cosmochim. Acta* 67, 2529-2542.

Li, D., Alidina, M., Ouf, M., Sharp, J.O., Saikaly, P., Drewes, J.E., (2013). Microbial community evolution during simulated managed aquifer recharge in response to different biodegradable dissolved organic carbon (BDOC) concentrations. *Water Res.* 47 (7), 2421-2430.

Liu, Y.-S., G.-G. Ying, A. Shareef, and R. S. Kookana, (2013), Biodegradation of three selected benzotriazoles in aquifer materials under aerobic and anaerobic conditions, *J. Contam. Hydrol.*, 151, 131–139.

Maeng, S.K., Sharma, S.K., Lekkerkerker-Teunissen, K., Amy, G.L., (2011). Occurrence and fate of bulk organic matter and pharmaceutically active compounds in managed aquifer recharge: a review. *Water Res.* 45 (10), 3015-3033.

Mariotti, A., Germon, J.C., Hubert, P., Kaiser, P., Letolle, R., Tardieux, P., (1981). Experimental determination of nitrogen kinetic isotope fractionation: some principles, illustration for the denitrification and nitrification processes. *Plant Soil* 62, 413-430.

Mariotti, A., Landreau, A., Simon, B., (1988). ^{15}N isotope biogeochemistry and natural denitrification process in groundwater application to the chalk aquifer of northern France. *Geochim. Cosmochim. Acta* 52, 1869-1878

Massmann, G., Greskowiak, J., Dunnbier, U., Zuehlke, S., Knappe, A., Pekdeger, A., (2006). The impact of variable temperatures on the redox conditions and the behaviour of pharmaceutical residues during artificial recharge. *J. Hydrol.*, 328 (1-2): 141- 156.

McIlvin, M.R., Altabet, M.A., (2005). Chemical conversion of nitrate and nitrite to nitrous oxide for nitrogen and oxygen isotopic analysis in freshwater and seawater. *Anal. Chem.* 77, 5589-5595.

Menció, A., Mas-Pla, J., Soler, A., Regàs, O., Boy-Roure, M., Puig, R., Bach, J., Domènech, C., Folch, A., Zamaroni, M., Brusi, D., (2016). Nitrate pollution of groundwater; all right..., but nothing else? *Sci. Total Environ.* 539C: 241-251.

Mengis, M., Schif, S.L., Harris, M., English, M.C., Aravena, R., Elgood, R.J, MacLean, A., (1999). Multiple geochemical and isotopic approaches for assessing ground water NO₃ elimination in a riparian zone. *Ground Water* 37, 448-457.

Miller, J.H., Ela, W.P., Lansey, K.E., Chipello, P.L., Arnold, R.G., (2006). Nitrogen transformations during soil-aquifer treatment of wastewater effluent-oxygen effects in field studies. *J. Environ. Eng. Asce* 132 (10): 1298-1306.

Otero, N., Soler, A., Canals, A., (2008). Controls of $\delta^{34}\text{S}$ and $\delta^{18}\text{O}$ in dissolved sulphate: learning from a detailed survey in the Llobregat River (Spain). *Appl. Geochm.* 23, 1166-1185.

Otero, N., Torrentó, C., Soler, A, Menció, A., Mas-Pla, J., (2009). Monitoring groundwater nitrate attenuation in a regional system coupling hydrogeology with multi-isotopic methods: the case of Plana de Vic (Osona, Spain). *Agric. Ecosyst. Environ.* 133 (1-2), 103-113.

Parkhurst, DL, Appelo, CAJ (2012) Description of input and examples for PHREEQC version 3a computer program for speciation, batch-reaction, one-dimensional transport, and inverse geochemical calculations. USGS Techniques and Methods, book 6, chap. A43, 497 p., available only at <http://pubs.usgs.gov/tm/06 A43/>.

Pauwels, H., Foucher, J.C., and Kloppmann, W. (2000). Denitrification and mixing in a schist aquifer: influence on water chemistry and isotopes. *Chem. Geol.* 168, 307-324.

Pauwels, H., Ayraud-Vergnaud, V., Aquilina, L., and Molénat, J. (2010). The fate of nitrogen and sulfur in hard-rock aquifers as shown by sulfate-isotope tracing. *Appl. Geochem.* 25, 105-115.

Pauwels, H., Kloppmann, W., Foucher, J.C., Martelat, A., and Fritsche, V. (1998). Field tracer test for denitrification in a pyrite-bearing schist aquifer. *Appl. Geochem.* 13, 284-292.

Patterson, B., Shackleton, M., Furness, A., Bekele, E., Pearce, J., Linge, K., Buseti, F., Spadek, T., Toze, S., (2011). Behaviour and fate on nine recycled water trace organics during managed aquifer recharge in aerobic aquifer. *J. Contam. Hydrol.* 122 (1-4), 53-62.

Pierre, C., Taberner, C., Urquiola, M.M., Pueyo, J.J., (1994). Sulphur and oxygen isotope composition of sulphates in hypersaline environments, as markers of redox depositional versus diagenetic changes. *Mineral Mag.* 58, 724-725.

Quevauviller, P.P., Fouillac, A.M., Grath, J., Ward, R., (2009). *Groundwater monitoring*, Wiley, New York. ISBN: 978-0-470-74969-2.

Rodríguez-Escales, P., Folch, A., van Breukelen, B.M., Vidal-Gavilan, G., Sanchez-Vila, X., (2016a). Modeling long term enhanced in situ biodenitrification and induced heterogeneity in column experiments under different feeding strategies. *J. Hydrol.* 538, 127-137.

Rodríguez-Escales, P., Folch, A., Vidal-Gavilan, G., van Breukelen, B.M. (2016b). Modeling biogeochemical processes and isotope fractionation of enhanced in situ biodenitrification in a fractured aquifer. *Chem. Geol.*, 425, 52-64.

Rodríguez-Escales, P., Fernández-García, D., Drechsel, J., Folch, A., Sanchez-Vila, X. (2017). Improving degradation of emerging organic compounds by applying chaotic advection in Managed Aquifer Recharge in randomly heterogeneous porous media. *Water Resour. Res.*, 53 (5), 4376-4392.

Ryabenko, E., Altabet, M.A., Wallace, D.W.R., (2009). Effect of chloride on the chemical conversion of nitrate to nitrous oxide for $\delta^{15}\text{N}$ analysis. *Limnol. Oceanogr.* 7, 545-552.

Schmidt, C.M., Fisher, A.T., Racz, A., Wheat, C.G., Los Huertos, M., Lockwood, B., (2012). Rapid nutrient load reduction during infiltration of managed aquifer recharge in an agricultural groundwater basin: Pajaro Valley, California. *Hydrol. Process.* 26, 2235-2247.

Schmidt, C.S., Richardson, D.J., Baggs, E.M., (2011). Constraining the conditions conducive to dissimilatory nitrate reduction to ammonium in temperate arable soils. *Soil Biol. Biochem.* 43, 1607-1611.

Sine S.E., (2017) Paradigm shift: does river metabolism mask the isotopic signal of nitrate sources? MSc. Thesis. University of Waterloo. 118 p.

Solà, V., (2009). Actualització hidroquímica i isotòpica dels aqüífers del Baix Llobregat per a la determinació de la intrusió marina, amb consideració de la isotopia del sulfat. Tesi de Màster en Hidrologia Subterrània.

Sprenger, C., Hartog, N., Hernández, M., Vilanova, E., Grützmacher, G., Scheibler, F., Hannappel, S., (2017) Inventory of managed aquifer recharge sites in Europe: historical development, current situation and perspectives. *Hydrogeol J*, 25, 1909-1922

Torrentó, C., Urmeneta, J., Otero, N., Soler, A., Viñas, M., Cama, J., (2011). Enhanced denitrification in groundwater and sediments from a nitrate-contaminated aquifer after addition of pyrite. *Chem. Geol.* 287, 90-101.

Utrilla, R., Pierre, C., Orti, F., Pueyo, J.J., (1992). Oxygen and sulphur isotope compositions as indicators of the origin of Mesozoic and Cenozoic evaporites from Spain. *Chem. Geol. Isot. Geosci.* 102, 229-244.

Valhondo, C., Carrera, J., Ayora, C., Barbieri, M., Noedler, K., Licha, T., Huerta, M., (2014). Behavior of nine selected emerging trace organic contaminants in an artificial recharge system supplemented with a reactive barrier. *Environ. Sci. Pollut. R.* 21, 11832-11843

Valhondo, C., Carrera, J., Ayora, Tubau, I., Martinez-Landa, L., Nödler, K., Licha, T., (2015). Characterizing redox conditions and monitoring attenuation of selected pharmaceuticals during artificial recharge through a reactive layer. *Sci. Total Environ.* 512-513, 240-250.

Valhondo, C., Martinez-Landa, L., Carrera, J., Hidalgo, J.J., Tubau, I., De Pourcq, K., Grau-Martínez, A., Ayora, C., (2016). Tracer test modeling for local scale residence time distribution characterization in an artificial recharge site. *Hydrol.Earth Syst.Sci.* 20, 4209-4221.

Valhondo, C., Martinez-Landa, L., Carrera J., Ayora, c., Nödler, K., Licha. T., (2018). Evaluation of EOC removal processes during artificial recharge through a reactive barrier. *Sci. Total Environ.* 612, 985-994.

Vanderzalm, J., Salle, C.L.G.L., Dillon, P., (2006). Fate of organic matter during aquifer storage and recovery (ASR) of reclaimed water in a carbonate aquifer. *Appl. Geochem.* 21 (7), 1204-1215.

Vázquez-Suñé, E., Capino, B., Abarca, E., Carrera, J., (2007). Estimation of recharge from floods in disconnected stream-aquifer systems, *Ground Water*, 45 (5), 579-589.

Vitòria, L., Otero, N., Canals, A., Soler, A., (2004). Fertilizer characterization: isotopic data (N, S, O, C and Sr). *Environ. Sci. Technol.* 38, 3254-3262.

Vogel, J.C., Ehhalt, D.H., (1963). The use of carbon isotopes in groundwater studies. In *Radioisotopes in Hydrology*. Vienna: International Atomic Energy Agency, pp. 338-396.

Xue, D., Botte, J., De Baets, B., Accoe, F., Nestler, A., Taylor, P., Van Cleemput, O., Berglund, M., Boeckx, P., (2009). Present limitations and future prospects of stable isotopes methods for nitrate source identification in surface and groundwater. *Water Res.* 43, 1159-1170.

Figure captions

Figure 1. Upper panel: Schematic location and plan view of the Sant Vicenç dels Horts recharge system. Lower panel: Cross-section of the transect A-A'. The red diamonds show the sampling depths.

Figure 2. Operational periods of the Sant Vicenç dels Horts MAR-PRL system between January 2013 and May 2015: recharge periods (RPs, blue) and non-recharge periods (NRPs, grey). The four sampling campaigns are also shown (red bars).

Figure 3. Changes in NO_3^- (A) and NO_2^- (B) concentrations over time in the batch experiments with compost extracted from the PRL (two-year-old reactive layer). Results of previous batch experiments with fresh commercial compost (Grau-Martínez et al., 2017) are also shown for comparison. Values and error bars represent the mean and standard deviation, respectively, for the experiments performed in triplicate.

Figure 4. N (A) and O (B) isotope results of the batch experiments performed with the two-year-old PRL material. Slopes of the regression lines represent $(\alpha-1)$ for N and O. Results of previous batch experiments with fresh commercial compost (Grau-Martínez et al., 2017) are also shown for comparison.

Figure 5. $\delta^{18}\text{O}\text{-H}_2\text{O}$ vs. $\delta^2\text{H}\text{-H}_2\text{O}$ of samples collected in June 2013 (RP) and July 2014 (RP) from the Llobregat River, native groundwater (P1) and mixed groundwater (all the piezometers, except P1). The Local Meteoric Water Line (LMWL) and weighted mean precipitation (WMP) are also shown, as well as the groundwater samples from the Llobregat aquifer collected in an area close to the MAR pond ("Llobregat aquifer", Solà, 2009) and Llobregat river samples collected in 1998-1999 ("LB", Otero et al., 2008).

Figure 6. Changes in the concentration of NPDOC and NO_3^- in depth-specific groundwater samples along the flow path under both RPs (a, c) and NRPs (b, d). Values for the Llobregat river samples are also shown. The size of the symbols is proportional to the corresponding concentration value. Concentrations ranged from 0.11 to 8.6 mg L^{-1} for NPDOC and from

0.01 to 19.4 mg L⁻¹ for NO₃⁻. Concentration values are given in the Supplementary Material (Table S3).

Figure 7. $\delta^{15}\text{N}_{\text{NO}_3}$ and $\delta^{18}\text{O}_{\text{NO}_3}$ of dissolved NO₃⁻ in the collected samples, as well as the isotope composition of the main nitrate sources: fertilizers, soil nitrate and animal manure or sewage (Vitòria et al., 2004; Kendall et al., 2007; Xue et al., 2009).

Figure 8. Estimation of the extent of NO₃⁻ attenuation in all the sampling campaigns, using ϵ values obtained from the batch experiments with two-year-old PRL material. The isotope composition of the native groundwater was used as the initial value.

Figure 9. $\delta^{18}\text{O}_{\text{SO}_4}$ vs $\delta^{34}\text{S}_{\text{SO}_4}$ for river, native groundwater and mixed groundwater samples collected in June 2013 and September 2013. The isotope composition of potential SO₄²⁻ sources is also shown. Values for SO₄²⁻ derived from sulfide oxidation are from Pierre et al. (1994) for disseminated pyrite in anoxic Tertiary marls that outcrop in the Llobregat River basin. Values for pig manure are taken from Otero et al. (2008) and Cravotta (1997). Soil SO₄²⁻ data are from Krouse and Mayer (2000) and fertilizer data from Vitòria et al. (2004). Gypsum values correspond to local gypsum outcrops (Utrilla et al., 1992). Sewage data are from the Igualada sewage plant (Otero et al., 2008).

Figure 10. $\delta^{13}\text{C}_{\text{HCO}_3}$ vs HCO₃⁻ concentration for native and mixed groundwater samples collected in June 2013, September 2013 and July 2014. The dotted lines represent the range of the $\delta^{13}\text{C}_{\text{HCO}_3}$ values for the native groundwater samples.

Figure 1

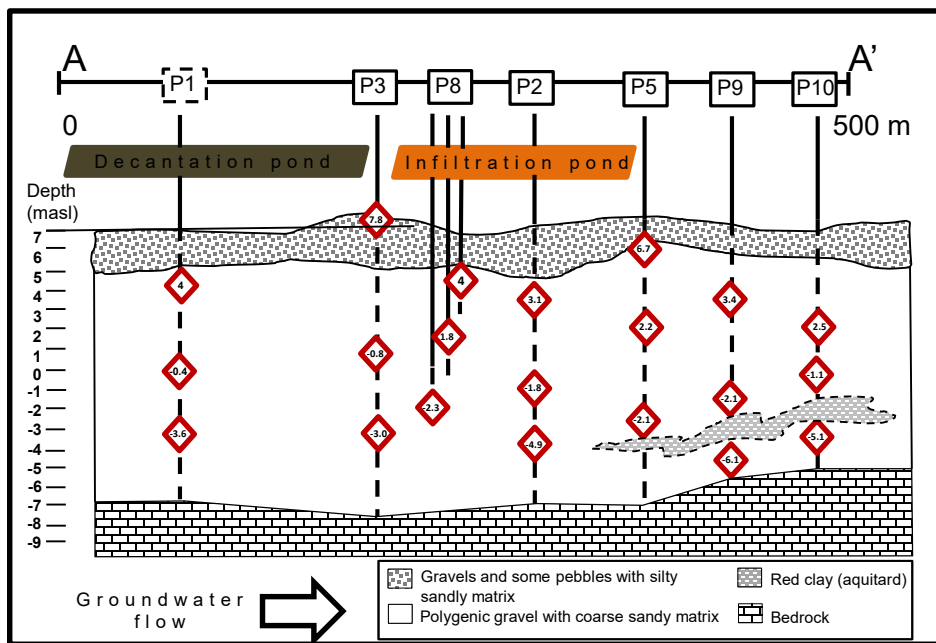
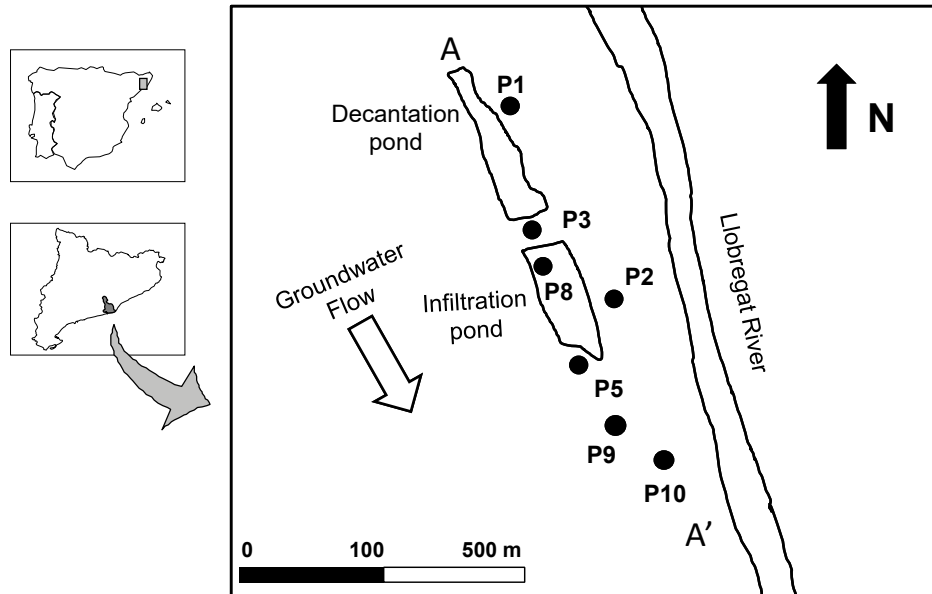
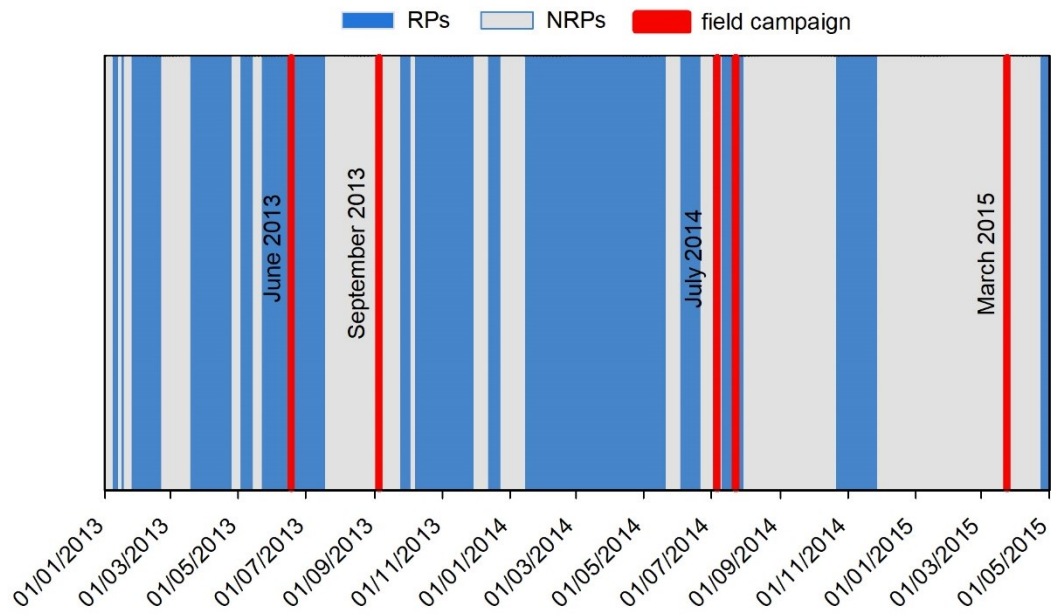


Figure 2



ACCEPTED

Figure 3

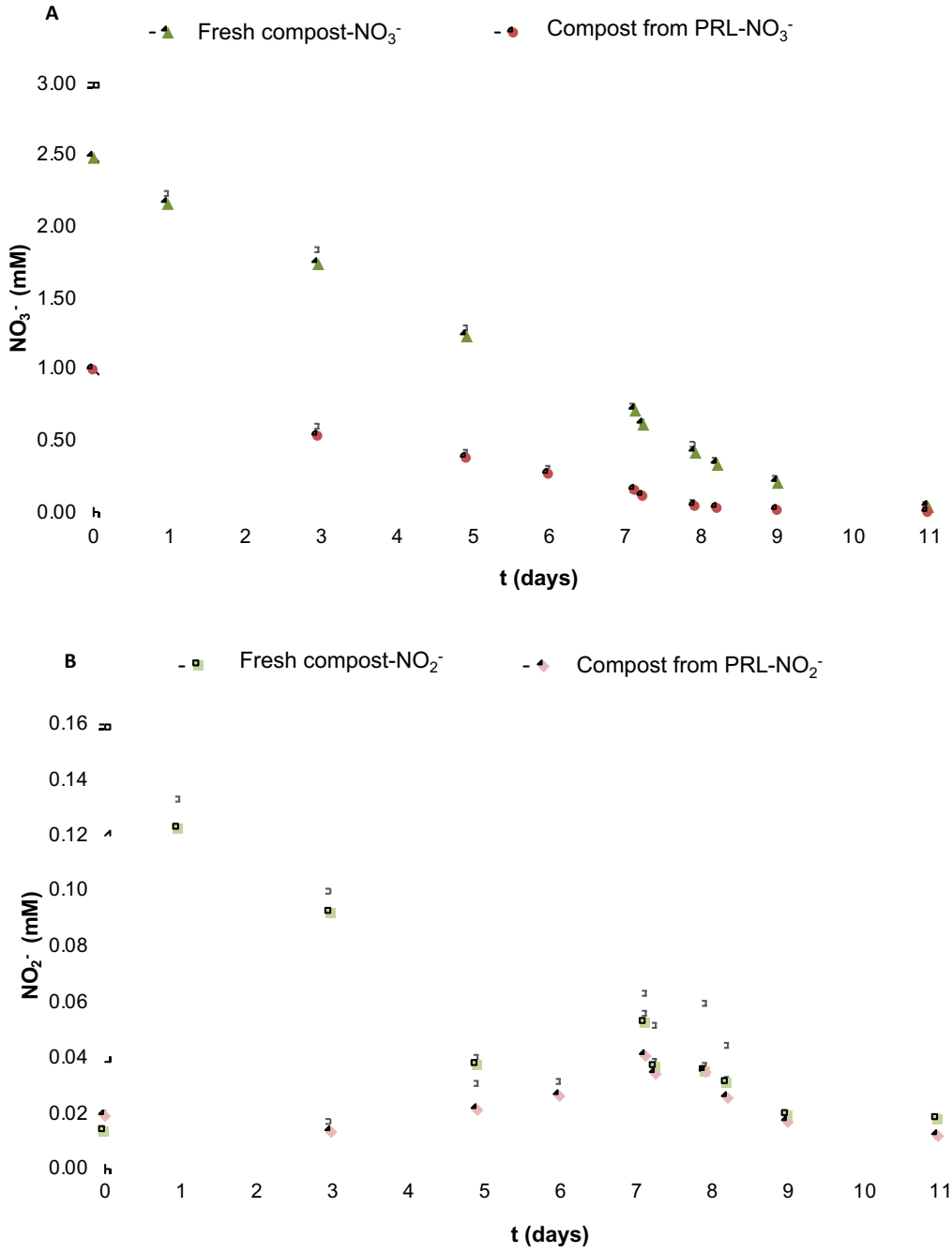


Figure 4

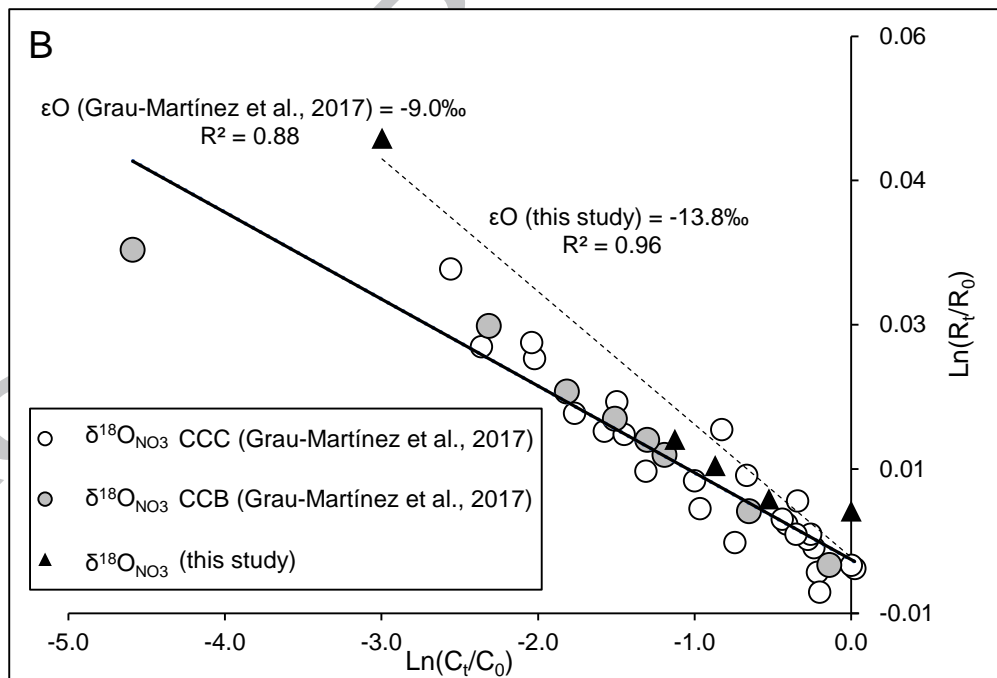
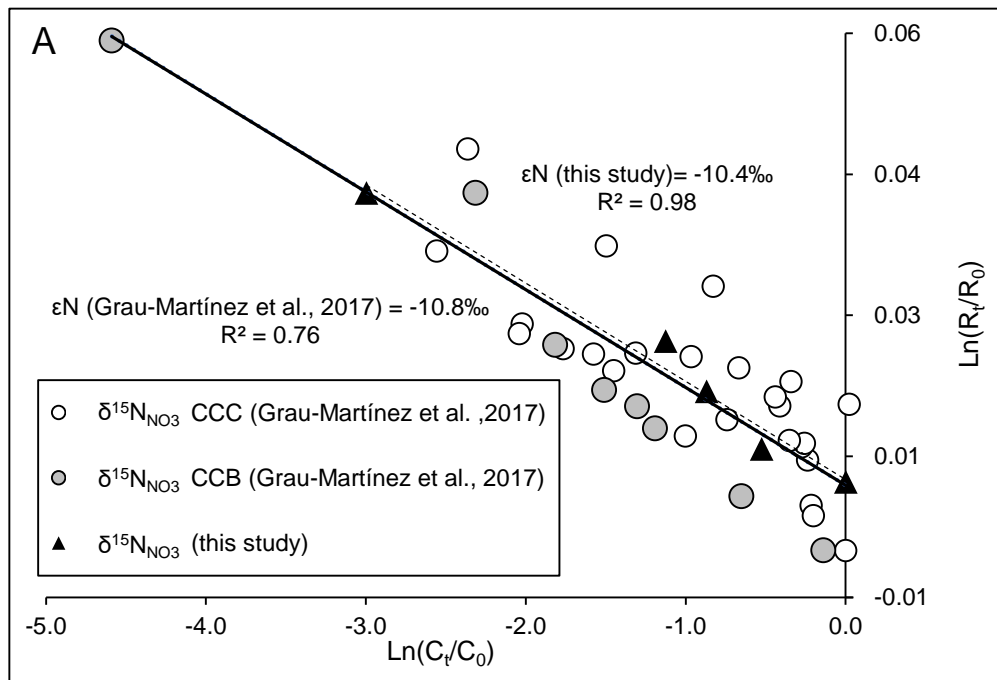


Figure 5

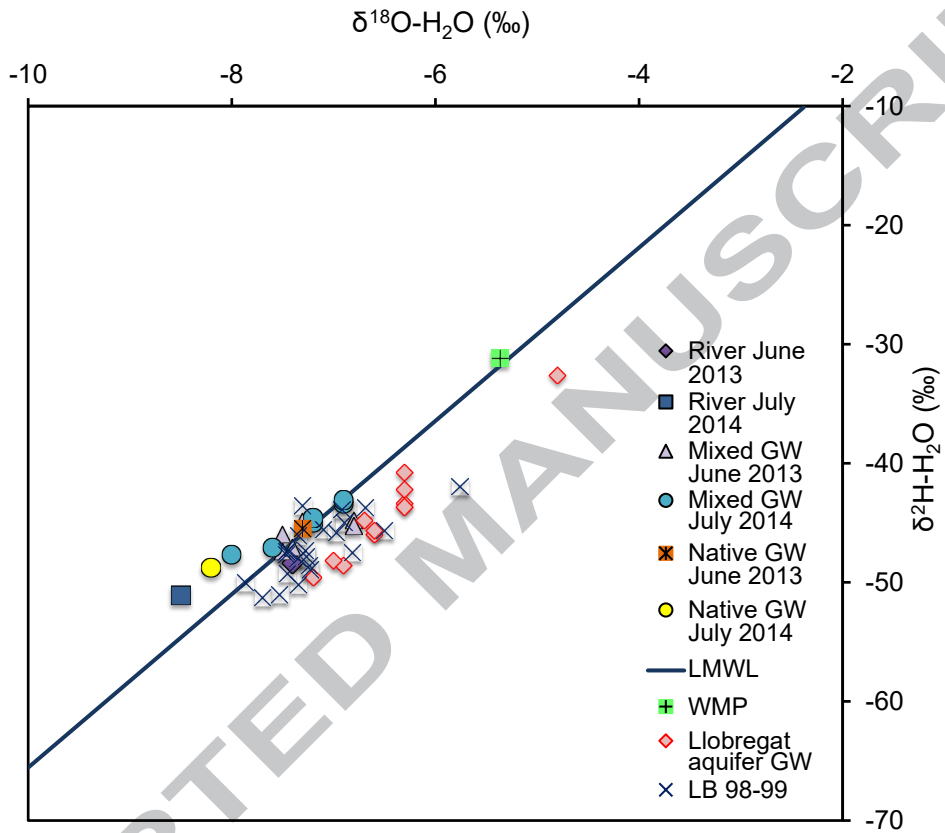


Figure 6

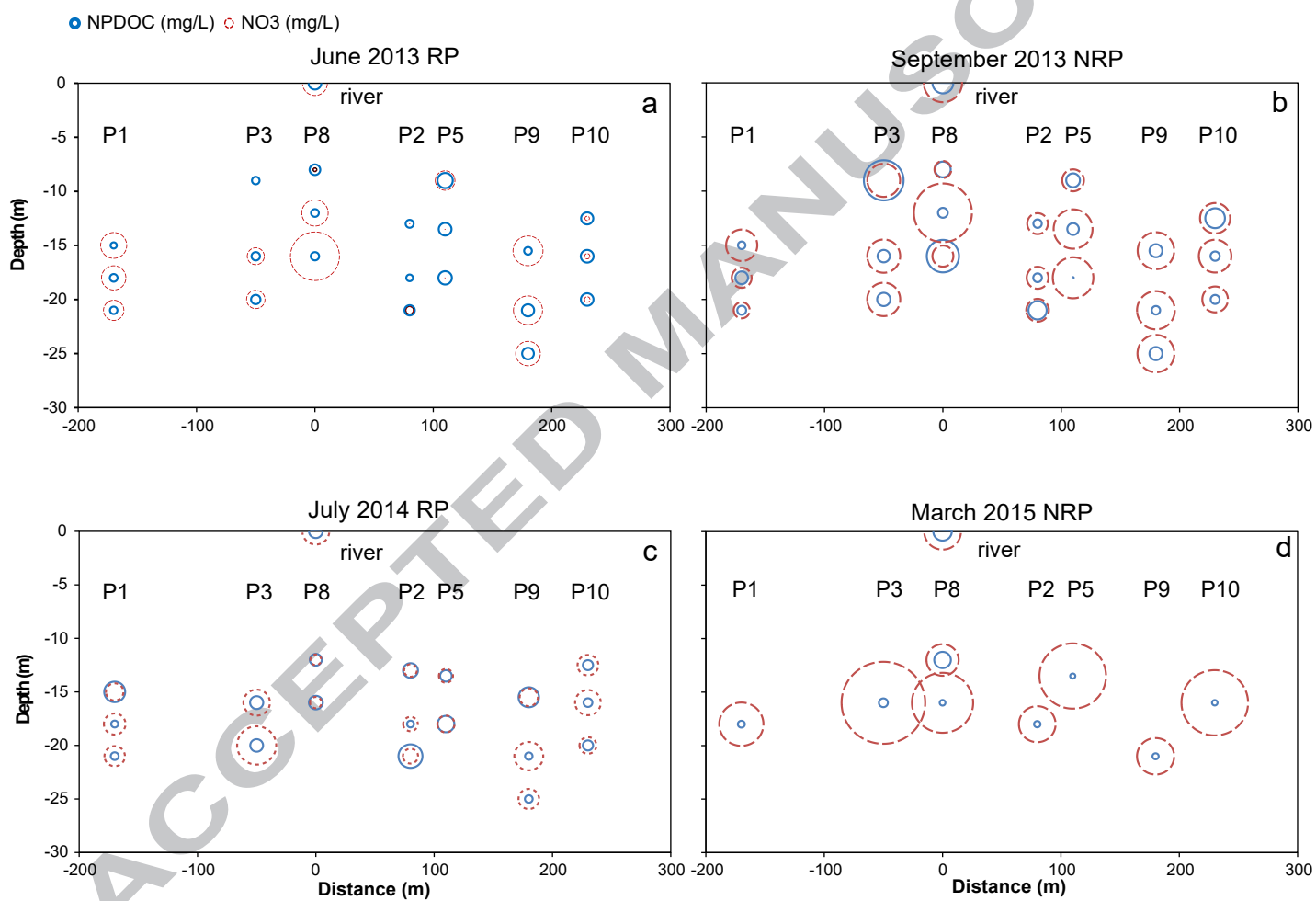


Figure 7

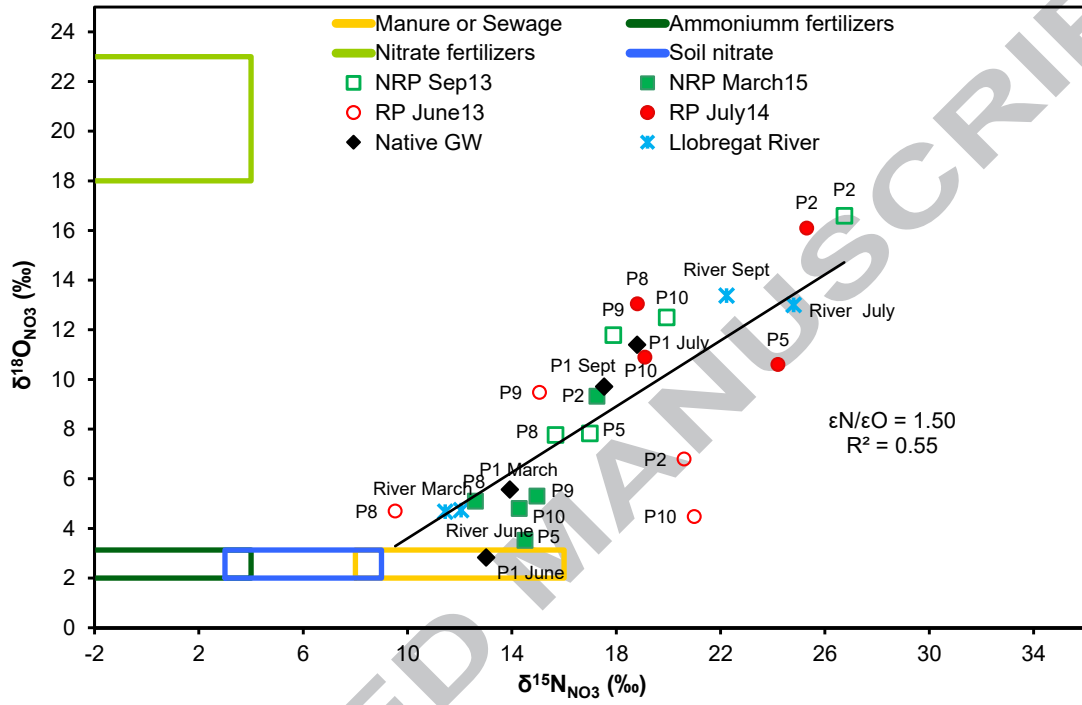


Figure 8

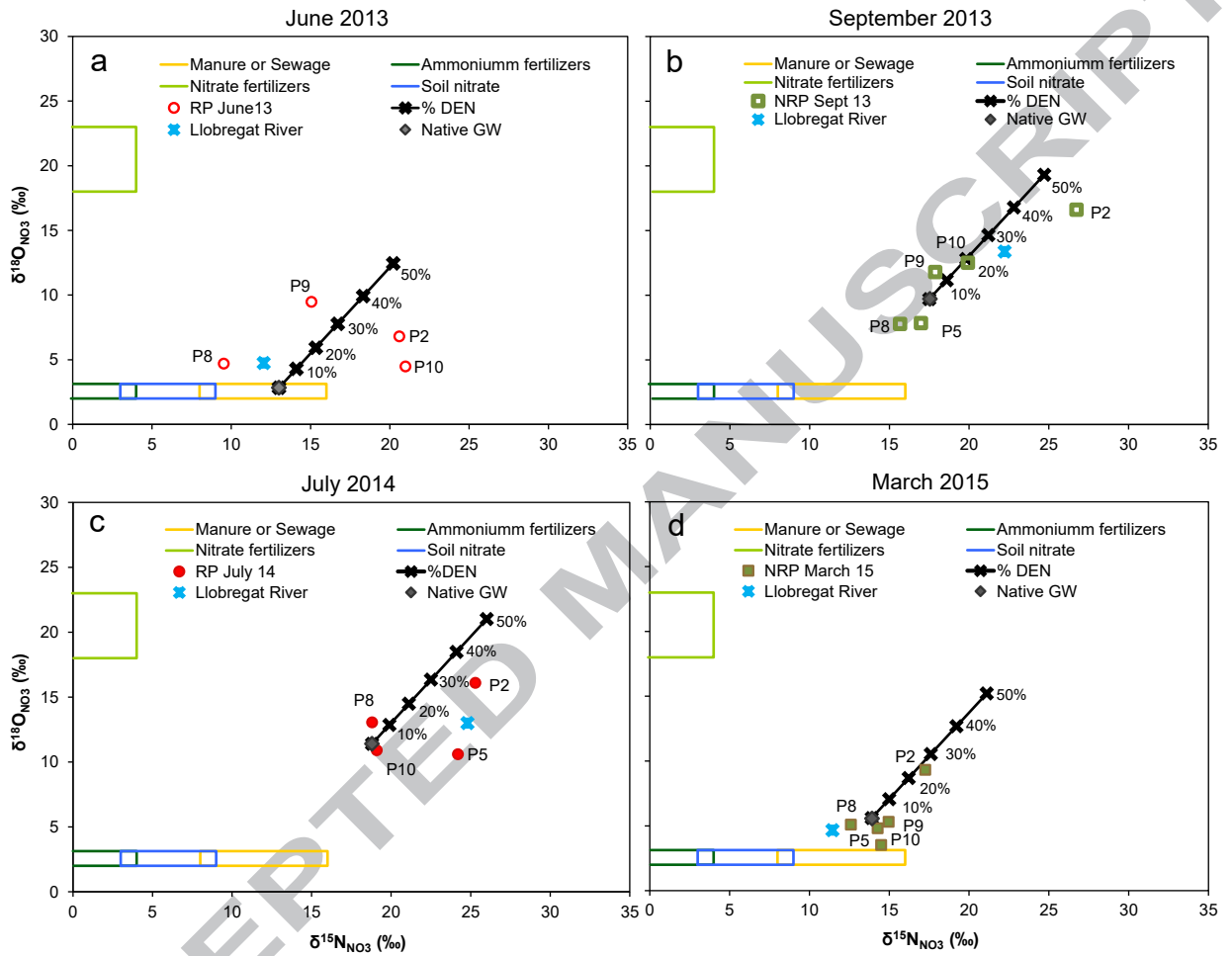


Figure 9

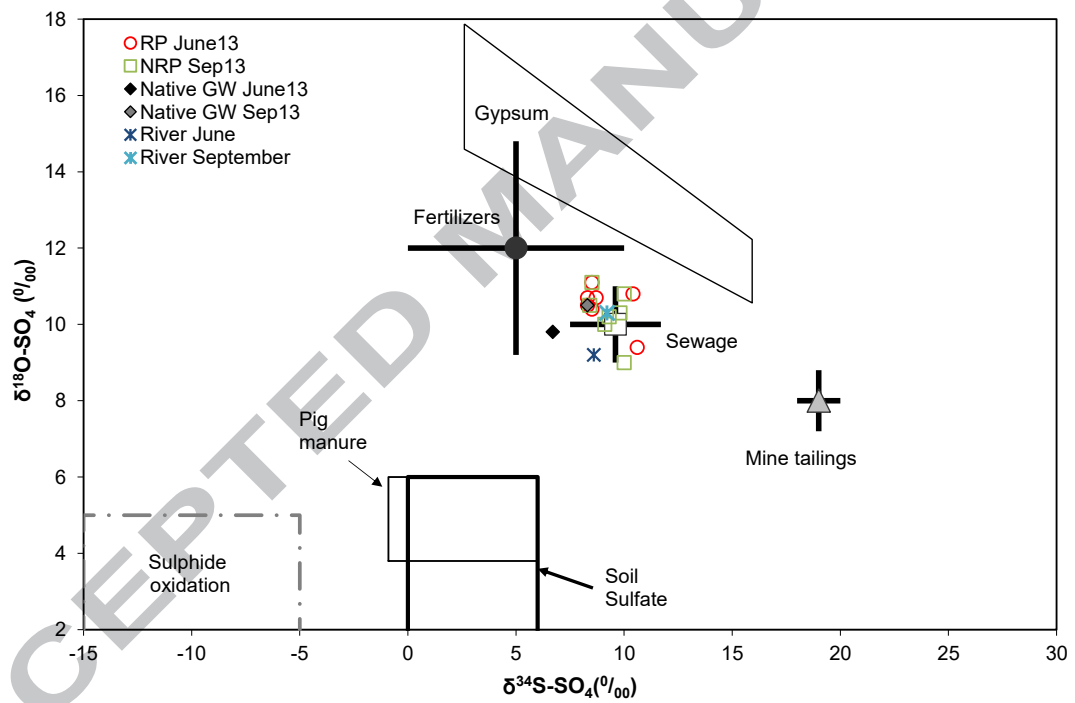
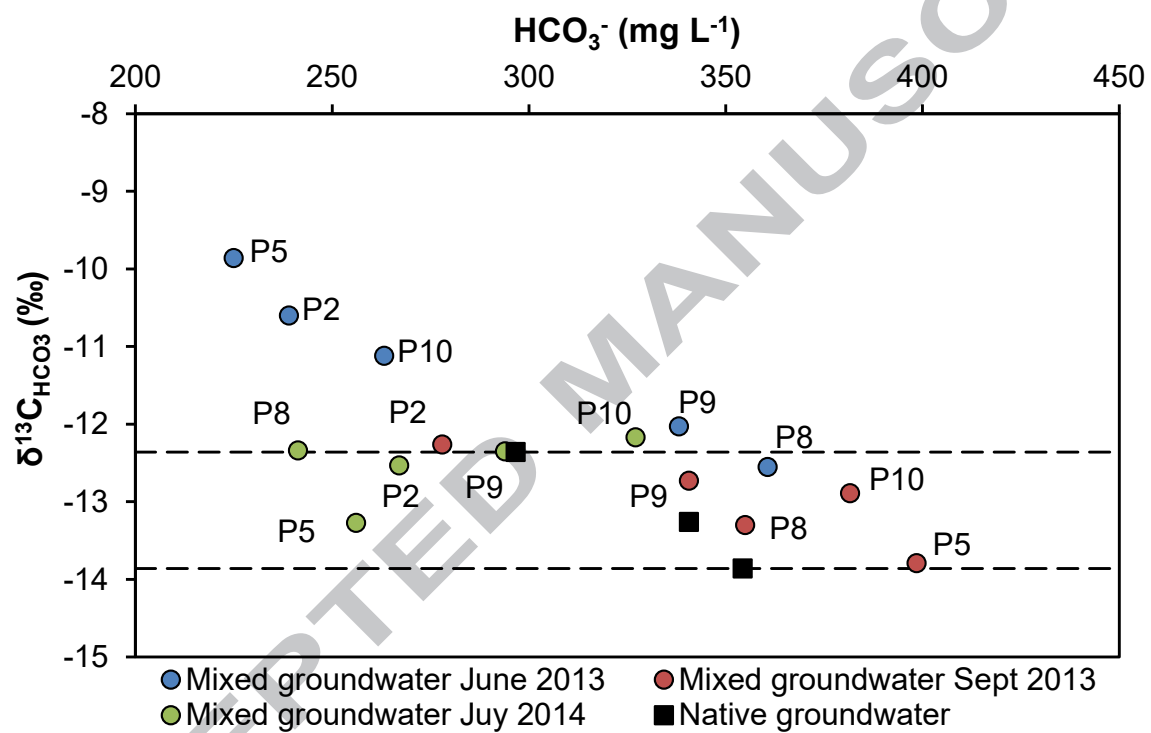


Figure 10



Highlights

Multi-isotope analysis was used to characterise a MAR pond.

A reactive layer installed in the MAR system to induce pollutants degradation is still working after 5 years.

Denitrification occurs mainly in the area where recharge water and groundwater mix.

The microbial community is still active even after a two-month non-recharge period.

Multi-isotope analysis might be useful in identifying and quantifying denitrification in MAR-PRL systems.

ACCEPTED MANUSCRIPT